

The Mueller-Tang jet impact factor at NLO from the high energy effective action

Martin Hentschinski* and Beatrice Murdaca†

**Instituto de Ciencias Nucleares, Universidad Nacional Autónoma de México, Apartado Postal 70-543, México Distrito Federal 04510, México*

†*Dipartimento di Fisica, Università della Calabria, and Istituto Nazionale di Fisica Nucleare, Gruppo collegato di Cosenza, I-87036 Arcavacata di Rende, Cosenza, Italy*

Abstract. We report on recent progress in the evaluation of next-to-leading order observables using Lipatov’s QCD high energy effective action. In this contribution we focus on the determination of the real part of the next-to-leading order corrections to the Mueller-Tang impact factor which is the only missing element for a complete NLO BFKL description of quark induced dijet events with a rapidity gap.

Keywords: High energy effective action, jets with rapidity gaps, diffraction, BFKL

PACS: 12.38.Bx, 12.38.Cy, 12.39.St

INTRODUCTION

Due to its large center of mass energy the LHC provides an ideal opportunity to test BFKL-driven observables [1, 2]. Among them both central production processes, such as heavy quark production [3], forward production of high p_T jets [4, 5] and Drell-Yan pairs [6, 7, 8, 9], and processes with hard events in both forward and backward direction, *i.e.* forward-backward (‘Mueller-Navelet’) jets [10] and forward Z boson production combined with a backward jet [11].

An observable of particular interest is given by forward/backward jets with a rapidity gap (‘Mueller-Tang’ jets). This process is special since it allows to probe the non-forward BFKL kernel, unlike the previously mentioned processes restricted to the forward case. From a phenomenological point of view the description in terms of the non-forward BFKL Green’s function is of relevance, since the latter describes a color singlet t -channel exchange. Unlike configurations which merely suppress emissions above a certain veto scale, the non-forward BFKL Green’s function therefore describes a t -channel exchange with emissions into the gap region intrinsically absent.

While the non-forward BFKL kernel is currently available at next-to-leading order (NLO) [12], only the virtual NLO corrections to the impact factors [13] are currently known; phenomenological studies, see *e.g.* [14, 15], are therefore limited to leading order (LO) impact factors. As NLO corrections to BFKL observables are often found to be size-able, this limitation to LO impact factors is currently one of the main drawbacks of BFKL phenomenology. A powerful tool to overcome this limitation is given by Lipatov’s effective action [16]. It is given in terms of the conventional QCD action to which a new induced term is added. The latter contains a new effective degree of freedom, the reggeized gluon, which has been introduced in order to achieve a gauge

invariant factorization of QCD amplitudes in the high energy limit. The determination of higher order corrections within this effective action is at first plagued by both technical and conceptual difficulties. Loop corrections show a new type of divergence, which is not present in usual QCD Feynman diagrams. Supplementing the QCD action with the additional induced term leads to an apparent over-counting problem. These problems have been addressed and resolved recently, first in the context of LO transition kernels [17, 18, 18, 20, 19] and later on in the calculation of NLO corrections to the forward quark-initiated jet vertex [21] and the quark contribution to the two-loop gluon trajectory [22], for a recent review see [23].

In this contribution we present some details of the determination of the missing real NLO correction to the quark-initiated Mueller-Tang jet impact factors. For further details and the complete result, including the gluon-initiated jet, we refer to [24].

THE HIGH ENERGY EFFECTIVE ACTION

The effective action adds to the QCD action an induced term, $S_{\text{eff}} = S_{\text{QCD}} + S_{\text{ind.}}$, which describes the coupling of the reggeized gluon field $A_{\pm}(x) = -it^a A_{\pm}^a(x)$ to the usual gluonic field $v_{\mu}(x) = -it^a v_{\mu}^a(x)$. This induced term reads

$$S_{\text{ind.}}[v_{\mu}, A_{\pm}] = \int d^4x \text{tr} \left[\left(W_+[v(x)] - A_+(x) \right) \partial_{\perp}^2 A_-(x) \right] + \int d^4x \text{tr} \left[\left(W_-[v(x)] - A_-(x) \right) \partial_{\perp}^2 A_+(x) \right]. \quad (1)$$

The infinite number of couplings of the gluon field to the reggeized gluon field are encoded in two functionals $W_{\pm}[v] = v_{\pm} \frac{1}{D_{\pm}} \partial_{\pm}$ where $D_{\pm} = \partial_{\pm} + gv_{\pm}$. Reggeized gluon fields are invariant under local $SU(N_c)$ gauge transformations. Strong ordering of longitudinal momenta in high energy factorized amplitudes provides the following kinematic constraint,

$$\partial_+ A_-(x) = \partial_- A_+(x) = 0, \quad (2)$$

which is always implied. Quantization of the gluonic field requires to add gauge fixing and ghost terms, which we have included in the QCD action. Feynman rules are given

FIGURE 1. From left to the right: the direct transition vertex, the reggeized gluon propagator and the order g induced vertex.

in Fig. 1. Curly lines describe the conventional QCD gluon field and wavy lines the reggeized gluon field. There exist an infinite number of higher order induced vertices.

For the present analysis only the order g induced vertex in Fig. 1 is needed. Loop corrections furthermore require a regularization of the light-cone singularity $1/k_1^\pm$. As discussed in [25] this pole should be treated as a Cauchy principal value.

MUELLER-TANG IMPACT FACTORS

The starting point for the determination of the quark induced Mueller-Tang jet impact factors is given by the quark-quark scattering amplitude with color singlet exchange. In the high energy limit such a scattering amplitude factorizes (in terms of a transverse convolution integral) into the two reggeized gluon exchange in the color singlet (which can be understood as the lowest order contribution to the perturbative Pomeron) and two impact factors (which describe the coupling of the two reggeized gluon state to the external quarks), see Fig. 2. Due to high energy factorization, the longitudinal part of the

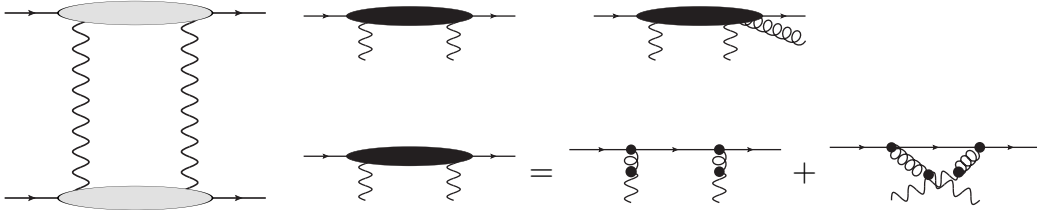


FIGURE 2. Left: Quark-quark scattering amplitude with exchange of two reggeized gluons in the color singlet. Right, top: leading and next-to-leading (real corrections) Mueller-Tang impact factor. Right, bottom: diagrammatic expansion of the LO impact factor.

loop integral *i.e.* the l^- (l^+) integration, can be entirely associated with the upper (lower) impact factor. At cross-section level, using dimensional regularization in $d = 4 + 2\varepsilon$ dimensions, the leading order result reads,

$$d\sigma_{ab} = H_a^{(0)} H_b^{(0)} \left[\int \frac{d^{2+2\varepsilon} l_1}{\pi^{1+\varepsilon}} \frac{1}{l_1^2(k-l_1)} \right] \left[\int \frac{d^{2+2\varepsilon} l_2}{\pi^{1+\varepsilon}} \frac{1}{l_2^2(k-l_2)} \right] d^{2+2\varepsilon} \mathbf{k} \quad (3)$$

with the impact factor

$$H_q^{(0)} = \frac{C_f^2}{N_c^2 - 1} \frac{N_c}{2N_c} \text{tr}(\not{p} \not{p}' \not{p} \not{p}') \frac{1}{2p_a^+} \cdot \frac{1}{p_a^+} \int \frac{dk^-}{2\pi} 2\pi \delta(k^- - \frac{\mathbf{p}^2}{p_a^+}) \frac{g^4}{2(4\pi)^{2+2\varepsilon}} \\ = \frac{\alpha_s^2 C_f^2}{\mu^{4\varepsilon} \Gamma^2(1-\varepsilon)(N_c^2 - 1)}, \quad (4)$$

in agreement with [26]. While the leading order impact factor is merely a constant, the real next-to-leading order corrections depend both on the momenta of the final state particles and the loop momentum of the reggeized gluon loop, l_1 and l_2 . Their integrated

version reads

$$\begin{aligned}
H_r^{(1)} = & \int_0^1 dz \int \frac{d^{2+2\varepsilon} \mathbf{q}}{\pi^{1+\varepsilon}} H^{(0)} \frac{\alpha_s}{2\pi} \frac{P_{qg}(z, \varepsilon)}{\Gamma(1-\varepsilon) \mu^{2\varepsilon}} \left[C_f \left(\frac{\Delta}{\Delta^2} - \frac{\mathbf{q}}{q^2} \right) \right. \\
& \left. - C_a \left(\frac{\mathbf{p}}{p^2} + \frac{1}{2} \frac{\Sigma_1}{\Sigma_1^2} + \frac{1}{2} \frac{\Upsilon_1}{\Upsilon_1^2} \right) \right] \left[C_f \left(\frac{\Delta}{\Delta^2} - \frac{\mathbf{q}}{q^2} \right) - C_a \left(\frac{\mathbf{p}}{p^2} + \frac{1}{2} \frac{\Sigma_2}{\Sigma_2^2} + \frac{1}{2} \frac{\Upsilon_2}{\Upsilon_2^2} \right) \right] \quad (5)
\end{aligned}$$

where $\Sigma_i = \mathbf{q} - \mathbf{l}_i$, $\Upsilon_i = \mathbf{q} - \mathbf{k} + \mathbf{l}_i$, and $i = 1, 2$. \mathbf{k} is the momentum transfer in the t -channel, \mathbf{q} the transverse momentum of the final state gluon. $P_{qg}(z, \varepsilon)$ is the real part of the $q \rightarrow g$ splitting function. For the limit $z \rightarrow 0$, the above expression can be shown to agree with the real part of the triple-Pomeron vertex [27, 18].

ACKNOWLEDGMENTS

We would like to thank G. Chachamis, J. Madrigal Martínez and A. Sabio Vera for fruitful collaboration. M.H. acknowledges support from the U.S. Department of Energy under contract number DE-AC02-98CH10886 and a BNL ‘‘Laboratory Directed Research and Development’’ grant (LDRD 12-034).

REFERENCES

1. V. S. Fadin, E. A. Kuraev and L. N. Lipatov, Phys. Lett. B **60** (1975) 50.
2. I. I. Balitsky and L. N. Lipatov, Sov. J. Nucl. Phys. **28** (1978) 822 [Yad. Fiz. **28** (1978) 1597].
3. G. Chachamis, M. Hentschinski, A. Sabio Vera and C. Salas, arXiv:0911.2662 [hep-ph].
4. M. Deak, F. Hautmann, H. Jung and K. Kutak, Eur. Phys. J. C **72** (2012) 1982 [arXiv:1112.6354 [hep-ph]].
5. F. Caporale, D. Y. Ivanov, B. Murdaca, A. Papa and A. Perri, JHEP **1202** (2012) 101 [arXiv:1112.3752 [hep-ph]].
6. F. Hautmann, M. Hentschinski and H. Jung, Nucl. Phys. B **865** (2012) 54 [arXiv:1205.1759 [hep-ph]].
7. F. Hautmann, M. Hentschinski and H. Jung, arXiv:1209.6305 [hep-ph].
8. F. Hautmann, M. Hentschinski and H. Jung, arXiv:1207.6420 [hep-ph].
9. F. Hautmann, M. Hentschinski and H. Jung, arXiv:1205.6358 [hep-ph].
10. D. Colferai, F. Schwennsen, L. Szymanowski and S. Wallon, JHEP **1012** (2010) 026 [arXiv:1002.1365 [hep-ph]].
11. M. Hentschinski, C. Salas, ‘‘Forward Drell-Yan and backward jet as a test of BFKL evolution’’, Proceedings of the XXth International Workshop on Deep-Inelastic Scattering and Related Subjects (DIS 2012), arXiv:1301.1227 [hep-ph].
12. V. S. Fadin and R. Fiore, Phys. Rev. D **72** (2005) 014018 [hep-ph/0502045].
13. V. S. Fadin, R. Fiore, M. I. Kotsky and A. Papa, Phys. Rev. D **61** (2000) 094006 [hep-ph/9908265], Phys. Rev. D **61**, 094005 (2000) [hep-ph/9908264].
14. O. Kepka, C. Marquet and C. Royon, Phys. Rev. D **83** (2011) 034036 [arXiv:1012.3849 [hep-ph]].
15. R. Enberg, G. Ingelman and L. Motyka, Phys. Lett. B **524** (2002) 273 [hep-ph/0111090].
16. L. N. Lipatov, Nucl. Phys. B **452** (1995) 369 [hep-ph/9502308].
17. M. Hentschinski, Nucl. Phys. Proc. Suppl. **198** (2010) 108 [arXiv:0910.2981 [hep-ph]].
18. M. Hentschinski, arXiv:0908.2576 [hep-ph].
19. M. Hentschinski, J. Bartels and L. N. Lipatov, arXiv:0809.4146 [hep-ph].
20. M. Hentschinski, Acta Phys. Polon. B **39** (2008) 2567 [arXiv:0808.3082 [hep-ph]].
21. M. Hentschinski and A. Sabio Vera, Phys. Rev. D **85** (2012) 056006 [arXiv:1110.6741 [hep-ph]].
22. G. Chachamis, M. Hentschinski, J. D. Madrigal Martinez and A. Sabio Vera, Nucl. Phys. B **861** (2012) 133 [arXiv:1202.0649 [hep-ph]], Nucl. Phys. B **876**, 453 (2013) [arXiv:1307.2591].

23. G. Chachamis, M. Hentschinski, J. D. Madrigal Martínez and A. Sabio Vera, Phys. Part. Nucl. **45**, no. 4, 788 (2014), arXiv:1211.2050 [hep-ph].
24. M. Hentschinski, J. D. Madrigal Martínez, B. Murdaca and A. Sabio Vera, Phys. Lett. **B735**, 168 (2014) arXiv:1409.6704 [hep-ph], Nucl. Phys. B **887**, 309 (2014) [arXiv:1406.5625 [hep-ph]], arXiv:1404.2937 [hep-ph].
25. M. Hentschinski, Nucl. Phys. B **859** (2012) 129 [arXiv:1112.4509 [hep-ph]].
26. A. H. Mueller and W. -K. Tang, Phys. Lett. B **284** (1992) 123.
27. J. Bartels and M. Wusthoff, Z. Phys. C **66** (1995) 157.